Jun 1st, 12:00 AM

Web Buckling in Beams

John T. DeWolf

Clinton J. Gladding

WEB BUCKLING IN BEAMS

by

John T. DeWolf[1] and Clinton J. Gladding[2]

INTRODUCTION

Webs of beams with large depth-thickness ratios are subject to buckling. Web crippling can occur at locations with concentrated loads or at supports. In regions of large shear, web buckling can occur due to the resulting compressive principal stress. Vertical buckling of the compressive flange into the web results from the bending deformations when the webs are too thin. The longitudinal compressive bending stresses can cause buckling. While each of these is well defined (6), design approaches are not always readily available, particularly for the last type. The "Specification for the Design, Fabrication and Erection of Structural Steel for Buildings" (8) has an approach which was developed for I-shaped plate girders and is thus not generally applicable to other sections. The "Specification for the Design of Cold-Formed Steel Structural Members" (9) does not fully consider the resulting postbuckling behavior.

Buckling due to the compressive bending stresses is of interest in this paper, with emphasis on the postbuckling strength. Previous work has included a theoretical and experimental study of box sections in which the agreement

---

[1] Asst. Prof. of Civil Engineering, The University of Connecticut, Storrs, Connecticut.

[2] Assistant Engineer, Northeast Utilities Service Company, Berlin, Connecticut.

between the two was lacking (3), an experimental investigation of aluminum plate girders (8), tests of steel plate girders which furnished information for the development of the first mentioned specification above (1), and an experimental study of box-type sections with a preliminary method proposed for predicting their strength (5).

This study has involved an experimental study of hat shaped sections with depth-thickness ratios between 136 and 364. From these an analytical approach has been developed based on determining the web effective width.

EXPERIMENTAL INVESTIGATION

Two sets of hat-shaped sections were tested, one with the neutral axis at the center of the web and one with it located so that 60% of the web was in compression. The cross-section is shown in Fig. 1. The sections were press-brake formed and consisted of two plates riveted together at the compression flange. Additionally, plates were riveted to the lower tension flange for the latter set. The dimension of the cross-sections are given in Table 1.

Carbon steel of a structural quality yielded at 37.8 ksi (260.4 x 10^3 MN/m^2) and had an ultimate stress of 50.3 ksi (346.6 x 10^3 MN/m^2). The elongation of a 2 in. (50.8 mm) gage length at rupture was 39%.

The beam was loaded equidistance from the ends as shown in Fig. 2. The length of the central portion, in pure flexure, was proportioned so that the web buckled in three half waves.

Web crippling was prevented by attaching channels vertically to the web at points of loading. Buckling due to the shear stresses in the end regions was prevented by spot welding additional plates to the section. Vertical buckling

of the compression flange was prevented by minimizing the area of the compression flange. Lateral bracing prevented lateral-torsional buckling.

Strain gages were applied on one web and the compression flange at the center of the beam. They were located in pairs on adjacent sides of the plate to measure the bending deformations and the average longitudinal stress in the plate. Additionally the web out-of-plane deformations were measured.

All failures were due to web buckling. As a consequence the compression flange buckled. In all subsequent calculations pertaining to the failure load, the area of the compression flange was reduced to an effective one so that the edge stress times the effective area produced the same resultant force. The effective area ranged from 82 to 92% of the full area.

The moments at failure, M_{exp}, are given in Table 2. If buckling had not occurred and the stress distribution at failure was distributed linearly with a maximum equal to the yield stress, the corresponding moments, referred to as M_y, would be as shown in the third column in Table 2. This shows clearly that plate buckling significantly reduces the strength, by as much as 60%. This is primarily attributable to buckling in the web since the reduction in the moment assuming flange buckling only, with the web fully effective, ranged from 5 to 9%. This was determined by using the reduced effective area of the compressive flange and the full area of the web and the tension flange so that $M_y = \sigma_y I_{eff}/c$, where σ_y is the yield stress, I_{eff} the resulting effective area, and c the distance to the extreme compression fiber.

The maximum compressive stress in the web at buckling, σ_{cr}, is shown in Table 2. This was determined by averaging the critical strains from the different pairs of strain gages on the compressive region in the web. The critical strain was taken as the maximum compressive strain in the gage on the convex side of the wave in the buckled plate. A linear flexural stress distribution was assumed at buckling. The moment determined from this, M_{cr}, is also listed. The ratios

of M_{exp}/M_{cr}, up to 4.0, show that the postbuckling range is substantial.

The web out-of-plane deformations just prior to failure ranged from approximately one quarter of the plate thickness to the full plate thickness for series A, and from approximately one-half to one and a half times the plate thickness for series B. The deeper sections yielded the larger values.

The behavior of the web in the postbuckling range is demonstrated from plots of the stresses on the web, Figs. 3-10. The stresses were determined by averaging the strains on opposite sides of the plate. The stress distributions with largest values at the web extremes were those just prior to failure. These demonstrate that at failure the stresses in the compressive portion of the web near the neutral axis decrease to approximately zero. The neutral axis shifts downward with this, resulting in a nonlinear stress distribution.

PROPOSED ANALYTICAL METHOD

Based on the behavior demonstrated from the stress distributions at failure, the section is reduced to an effective one as shown in Fig. 11. The compression flange is also reduced, as noted previously. The resulting compressive and tensile stress distributions are linear.

The effective depth of the compression region was determined experimentally and listed in Table 3 as a_{exp}. This was done by equating the actual internal moment distribution on the web with that for the assumed distribution. The range in effective widths a_{exp} is considerably smaller than the range in depths d for the sections. For series A, the depth of section A4 is 2.0 times that for A1 while the ratio of the effective widths is only 1.27. For series B, the ratio of the depths of B4 to B1 is 2.67 and the ratio of the effective widths is 1.17.

It is assumed that at failure, the effective width expression should be a function of $\sqrt{\sigma_{cr}/\sigma_{max}}$, where σ_{max} is the maximum stress, equal to σ_y. This

follows from effective width expressions utilized for uniformly compressed plates (10,11). Additionally it has been assumed that the effective width for the web can be expressed in terms of the depth of the web compression zone prior to web buckling, d_o, rather than the entire depth. For determining d_o, the compression flange is fully effective since buckling has not occurred. These assumptions are at least partially verified when $a_{exp}/\sqrt{\sigma_{cr}/\sigma_y}$ is plotted versus d_o, shown in Fig. 12. The test critical stress was used for σ_{cr}. The relationship between these terms can be approximated by assuming a linear relationship, shown as the solid line. The best fit is obtained with a slope equal to 0.7. The resulting effective width for webs in pure flexure is then:

$$\frac{a}{d_o} = 0.7 \sqrt{\frac{\sigma_{cr}}{\sigma_y}} \qquad (1)$$

Values of a determined from Eq. (1) using the test σ_{cr} value and σ_y = 37.8 ksi (260.4 MN/m^2) are given in Table 3. The maximum variation from the test value was 12% and the mean 6%.

Using a determined from Eq. (1), the neutral axis location is calculated by equating the first moment of the area of the compression zone about the neutral axis with that of the tension zone. The maximum tensile stress, σ_t, is then calculated so that the internal compressive and tensile resultant forces are equal. The resulting moment is then calculated from the resulting stress distribution.

Values of d', the width of the web compression zone for the effective section, σ_t, and the predicted ultimate moment, M, are given in Table 4. With the exception of Specimen B4, all predictions are within 10% of the test ultimate moments. It is felt that possible imperfections in the manufacture of B4 induced initial stresses which led to premature failure.

Since only a limited number of tests were used in the establishment of a, possible refinement could result from additional tests. As an indication of what effect this would have on the resulting moment, a was arbitrarily varied 10%. The resulting moments are listed in Table 5. The variation in M is equal or less than 4%, demonstrating that for sections in which the web comprises a major portion of the cross-sectional area, the precise determination of a is not so important.

DESIGN SIMPLIFICATION

In design situations, σ_{cr} can not be determined from tests, but must be calculated. The classical critical stress for plates is:

$$\sigma_{cr} = k \frac{\pi^2 E}{12(1-\nu^2)\left(\frac{d}{t}\right)^2} \qquad (2)$$

in which E is the modulus of Elasticity, ν Poisson's ratio, d the plate width, or web depth here, and k a factor which depends on the manner in which the plate is supported along the edges in the direction of the compressive stress and the location of the neutral axis in the case of non-uniformly compressed elements. Conservative values of k, associated with simply supported edges, are used in design. Approximate simply supported values are 23.9 for series A and 15.7 for series B (2).

For steel, E is approximately 29,500 kips per square inch (2.03×10^5 MN/m^2), and ν is approximately 0.3. Substituting these values into Eq. (2) and then substituting this into Eq. (1) yields:

$$\frac{a}{d_o} = 114.3 \frac{t}{d} \sqrt{\frac{k}{\sigma_y}} \qquad (3)$$

Since d_o is equal to 0.5 d for series A and 0.6 d for series B, a is not a function of the element depth-thickness ratios for the separate series. This is consistent with the small variation in the effective width, a, shown in the test results. Note that the constant k varied due to the variation in the relative width-thickness ratios of the web and flanges.

The limiting web depth-thickness ratio, below which the section is fully effective, is obtained by setting $a = d_o$ in Eq. (3) and solving for d/t:

$$\left(\frac{d}{t}\right)_{lim} = 114.3 \sqrt{\frac{k}{\sigma_y}} \qquad (4)$$

Thus for web depths exceeding that in Eq. (4), the effective compression zone is determined from Eq. (3) assuming a simply supported value of k. The location of the neutral axis as shown in Fig. 11 is then determined so that the first moments of the areas of the tension and compression zones about the axis are equal. The maximum tensile stress is then calculated so that the resultant forces on the cross-section are equal. The resulting stress distribution then establishes the ultimate moment.

Values of the effective width, a, were determined using the simply supported k values and are presented in Table 3. These values are equal to or smaller than those determined from the test results, with a mean variation of 16.7%. The critical stresses for the plates used in determining the values of a and the resulting ultimate moments are given in Table 6. The maximum variation between the predicted and test values is 15%, and the mean variation is 10.6%.

CONCLUSIONS

Tests of hat-shaped sections in which the web buckles due to the flexural stresses have shown: (1) Web buckling considerably reduces the flexural strength;

(2) The postbuckling range is substantial and can be utilized in design since the out-of-plane deformations are not so large.

A conceptually simple method is proposed for predicting the ultimate moment for beams. The section is reduced to an effective one by assuming that a portion of the web compression zone nearest the neutral axis is ineffective. An empirical expression based on present effective width concepts is given which is a function of the critical stress, the yield stress and the depth of the web compression zone. The method is not limited to the cross-section studied.

Additional tests could lead to refinement in the effective width expression.

ACKNOWLEDGEMENT

The research described in this paper was supported by the National Science Foundation, Grant Number ENG75-10299.

APPENDIX I. REFERENCES

1. Bunler, K. and Thürlimann, B., "Strength in Bending," Transactions ASCE, Vol. 128, 1963, pp. 655-682.

2. Bleich, F., Buckling Strength of Metal Structures, McGraw-Hill Book Company, Inc., New York, 1952.

3. Chapman, J. C., "Behavior in Pure Bending of Box Girders," The Engineer, Vol. 198, Aug., 1954, pp. 253-257.

4. Johnson, A. L., "The Structural Performance of Austenitic Stainless Steel Members," Report No. 327, Department of Structural Engineering, Cornell University, Ithaca, N. Y., November, 1966.

5. LaBoube, R. A. and Yu, Wei-Wen, "Study of Cold-Formed Steel Beam Webs Subjected to Bending Stress," Publication of the Third International Speciality on Cold-Formed Steel Structures, St. Louis, Missouri, 1975, pp. 315-335.

6. McGuire, W., Steel Structures, Prentice-Hall, Inc., Englewood Cliffs, N.J., 1968.

7. Rockey, K. C., and Jenkins, P., "The Behaviour of Webplates of Plate Girders Subjected to Pure Bending," The Structural Engineer, Vol. 35, May 1957, pp. 176-189.

8. Specification for the Design, Fabrication and Erection of Structural Steel for Buildings, 1969 ed., American Institute of Steel Construction, New York, N.Y., 1969.

9. Specification for the Design of Cold-Formed Steel Structural Members, American Iron and Steel Institute, New York, N. Y., 1968.

10. von Karman, T., Sechler, E. E., and Donnell, L. H., "The Strength of Thin Plates in Compression," Transactions ASME, Vol. 54, 1932, pp. 53-57.

11. Winter, G., "Thin-Walled Structures -- Theoretical Solutions and Test Results," Preliminary Publication of the Eighth Congress, International Association for Bridge and Structural Engineering, 1968, pp. 101-112.

APPENDIX II. NOTATION

a = predicted effective width of web compression zone;

a_{exp} = effective width of web compression zone from tests;

b = width of tension in flange;

c = distance from neutral axis to extreme fiber;

d = depth of section;

$(d/t)_{lim}$ = maximum web depth thickness ratio for which the web is fully effective;

d_o = depth of web compression zone prior to buckling;

d' = predicted depth of web compression zone at failure;

E = modulus of elasticity (assumed as 29500 ksi);

h = clear distance between flanges;

I_{eff} = moment of inertia for full web and tension flange, effective portion of compression flange;

k = edge support coefficient for plate buckling;

M = predicted ultimate moment;

$M_{0.9}$ = ultimate moment for a equal to 0.9 a from Eq. (1);

$M_{1.1}$ = ultimate moment for a equal to 1.1 a from Eq. (1);

M_{cr} = moment at which the web buckled in tests;

M_{exp} = moment at failure for test specimens;

M_y = moment predicted assuming no plate buckling;

t = plate thickness;

t_a = thickness of additional tension flange area;

σ_{cr} = critical web stress, at junction with compression flange;

σ_{max} = maximum stress in web compression zone;

σ_t = predicted maximum stress in web tensile zone at failure;

σ_y = yield stress;

ν = Poisson's ratio

TABLE 1.

Cross-Section Dimensions

Specimen	t, in inches	t_a, in inches	b, in inches	d, in inches	Web depth-thickness ratio, h/t
A1	0.066	0.0	8.3	12	179
A2	0.066	0.0	8.3	16	240
A3	0.066	0.0	8.3	20	301
A4	0.066	0.0	8.3	24	361
B1	0.066	0.066	7.8	9	134
B2	0.066	0.132	6.0	14	210
B3	0.066	0.132	6.8	19	285
B4	0.066	0.132	7.8	24	361

Note: 1 inch = 25.4 mm

TABLE 2. - Test Moments

Specimen	Test failure moment, M_{exp}, in inch-kips	Failure Moment assuming no buckling, M_y, in inch-kips	M_{exp}/M_y	Critical stress, σ_{cr}, in kips per square inch	Test critical moment, M_{cr}, in inch-kips	M_{exp}/M_{cr}
A1	216	283	0.76	22	168	1.29
A2	306	430	0.71	15	162	1.89
A3	391	605	0.65	10	133	2.94
A4	464	806	0.58	8	118	3.93
B1	150	213	0.70	30	125	1.20
B2	287	410	0.70	13	139	2.06
B3	360	660	0.55	9	90	4.00
B4	389	974	0.40	6	110	3.54

Note: 1 inch-kip = 113 N·m; 1 kip per square inch = 6.89 MN/m^2.

TABLE 3. - Effective Widths

Specimen	Test effective width, a_{exp}, in inches	Effective width determined from Eq. 1 with test σ_{cr}		Effective width determined from Eq. 1 with σ_{cr} assuming simply supported edges	
		a, in inches	a/a_{exp}	a, in inches	a/a_{exp}
A1	3.0	3.1	1.03	3.0	1.00
A2	3.8	3.5	0.92	3.0	0.79
A3	3.7	3.6	0.97	3.0	0.81
A4	3.4	3.8	1.12	3.0	0.88
B1	3.6	3.3	0.92	2.9	0.81
B2	3.5	3.4	0.97	2.9	0.83
B3	3.5	3.8	1.09	2.9	0.83
B4	4.1	4.0	0.98	2.9	0.71

Note: 1 inch = 25.4 mm

TABLE 4. - Ultimate Moment Capacity

Specimen	Distance to neutral axis at failure, d', in inches	Maximum tensile stress, σ_t, in kips per square inch	Predicted ultimate moment, M, in inch-kips	Test ultimate moment, M_{exp}, in inch-kips	M/M_{exp}
A1	6.5	26.0	201	216	0.93
A2	8.9	23.7	280	306	0.92
A3	11.4	21.4	355	391	0.91
A4	13.9	20.1	440	464	0.95
B1	5.7	18.4	161	150	1.07
B2	9.3	15.2	258	287	0.90
B3	12.9	13.5	372	360	1.03
B4	16.9	11.7	481	389	1.24

Note: 1 inch = 25.4 mm; 1 kip per square inch = 6.89 MN/m^2; 1 inch-kip = 113 N·m

TABLE 5. - Effect of Varying Effective Width

Specimen	$\frac{a}{d_o} = 0.9\left[0.7\sqrt{\frac{\sigma_{cr}}{\sigma_y}}\right]$			$\frac{a}{d_o} = 1.1\left[0.7\sqrt{\frac{\sigma_{cr}}{\sigma_y}}\right]$		
	a in inches	$M_{0.9}$ in inch-kips	$^*M_{0.9}/M$	a in inches	$M_{1.1}$ in inch-kips	$^*M_{1.1}/M$
A1	2.8	194.3	0.96	3.5	208.1	1.03
A2	3.1	269.4	0.96	3.8	290.0	1.04
A3	3.2	340.9	0.96	3.9	367.9	1.04
A4	3.4	421.8	0.96	4.2	456.9	1.04
B1	3.0	155.1	0.96	3.6	166.0	1.03
B2	3.1	248.5	0.96	3.7	267.8	1.04
B3	3.5	356.8	0.95	4.2	387.0	1.04
B4	3.6	460.5	0.95	4.4	501.1	1.04

*M given in Table 4.

Note: 1 inch = 25.4 mm; 1 inch-kip = 113 N·m

TABLE 6. - Ultimate Moments Determined According to Design Simplification

Specimen	Critical stress, σ_{cr}, in kips per square inch	Distance to neutral axis at failure, d', in inches	Maximum tensile stress, σ_t, in kips per square inch	Predicted ultimate moment, M, in inch-kips	Test ultimate moment M_{exp} in inch kips	M/M_{exp}
A1	19.7	6.5	25.5	198	216	0.91
A2	11.1	9.0	22.5	265	306	0.87
A3	7.0	11.7	20.3	332	391	0.85
A4	4.9	14.4	18.6	400	464	0.86
B1	23.7	5.8	17.6	155	150	1.03
B2	9.7	9.5	14.4	245	287	0.85
B3	5.2	13.4	12.2	335	360	0.93
B4	3.3	17.6	10.4	426	389	1.09

Note: 1 kip per square inch = 6.89 MN/m^2; 1 inch = 25.4 mm; 1 inch-kip = 113 N·m

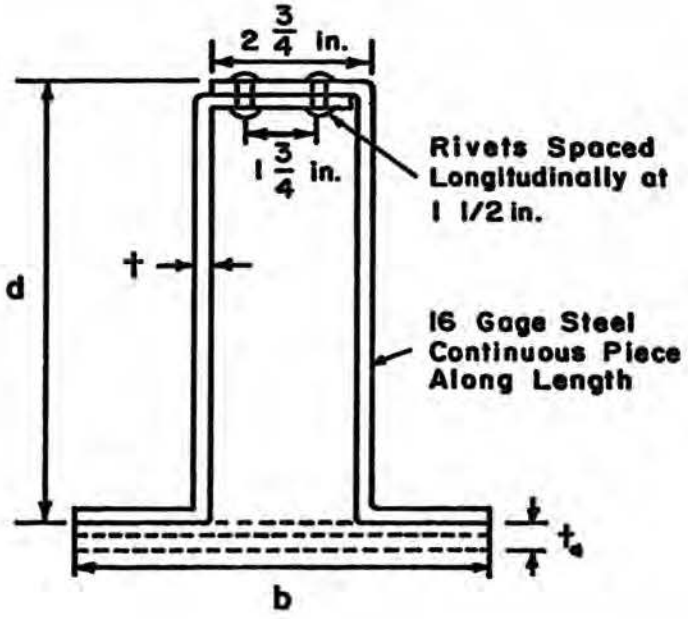

FIG. 1. - Cross Section of Test Specimen in Region of Flexure Only

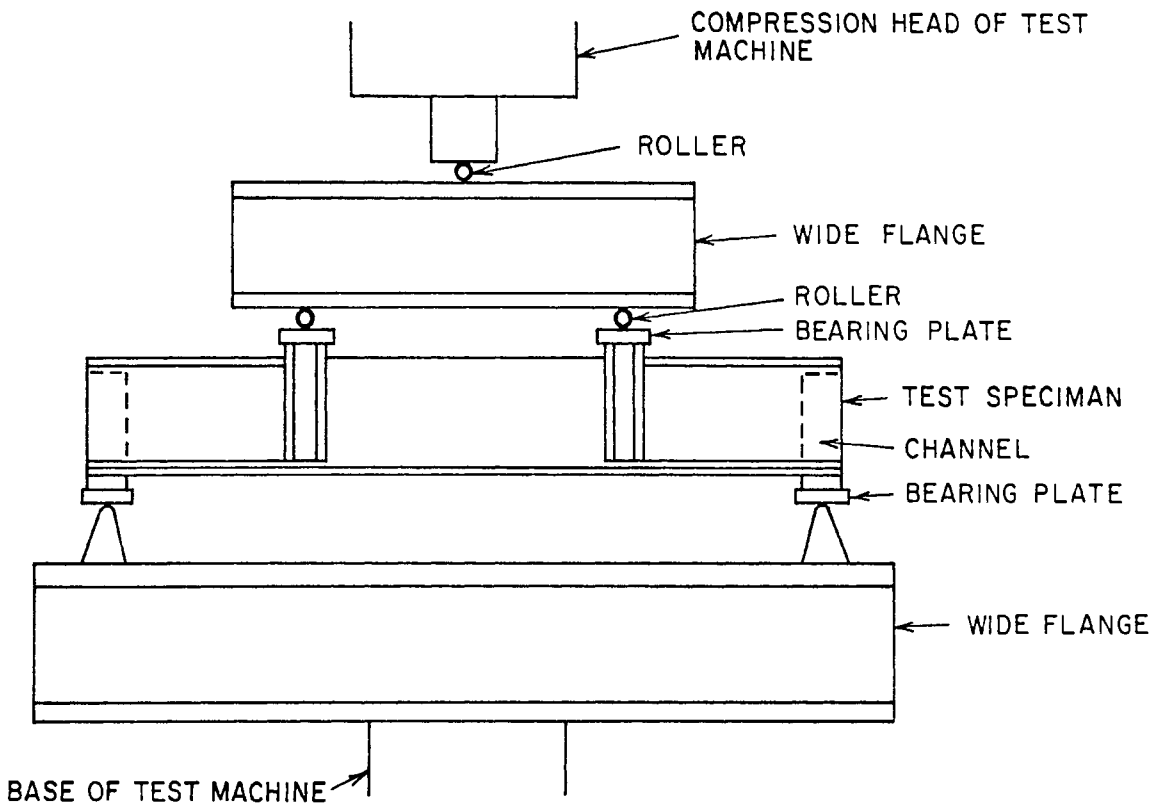

FIG. 2. - Loading Arrangement

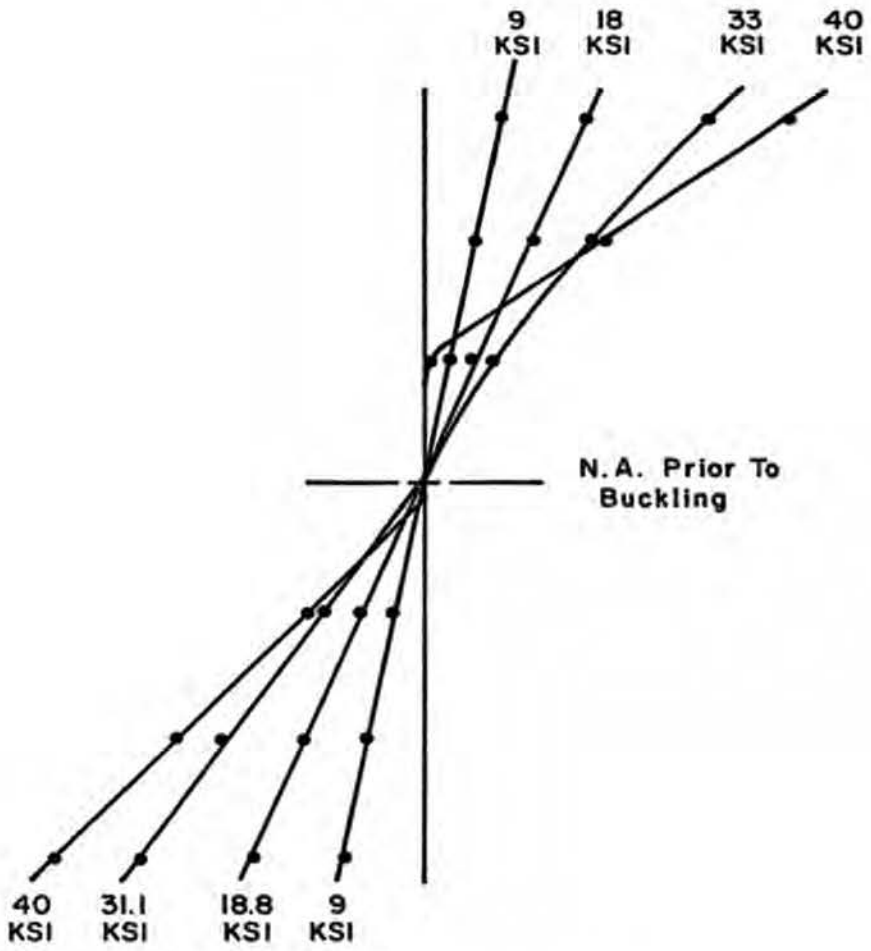

FIG. 3. - Web Stress Distributions at Loads Equal to 24, 51, 78, and 100 % of Ultimate Load for Specimen A1 (h/t = 179)

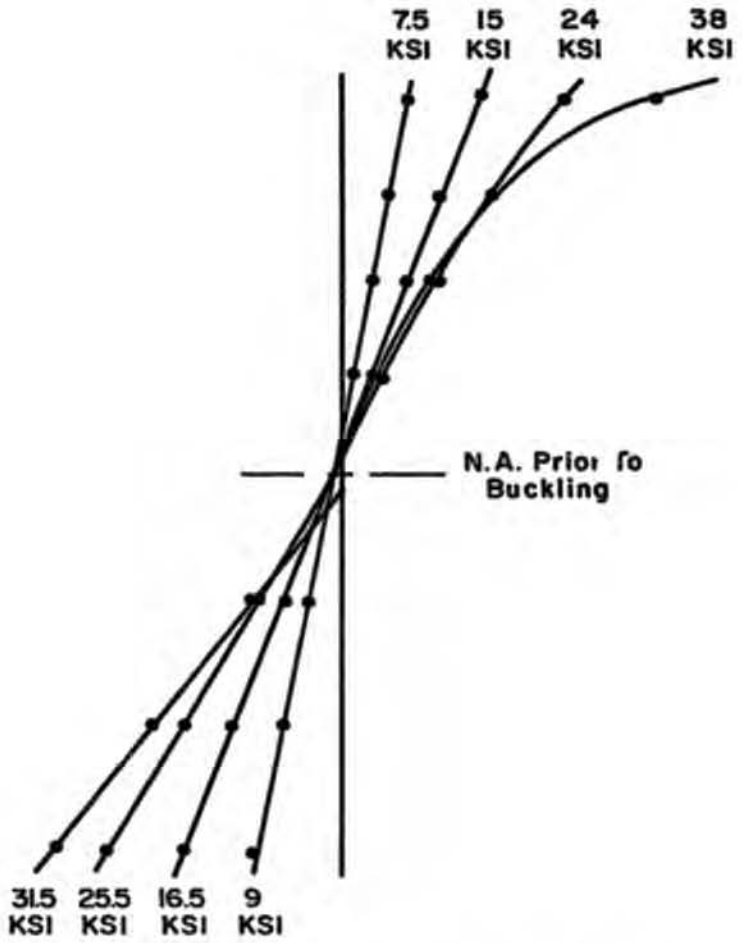

FIG. 4. - Web Stress Distributions at Loads Equal to 26, 53, 79, and 100 % of Ultimate Load for Specimen A2 (h/t = 240)

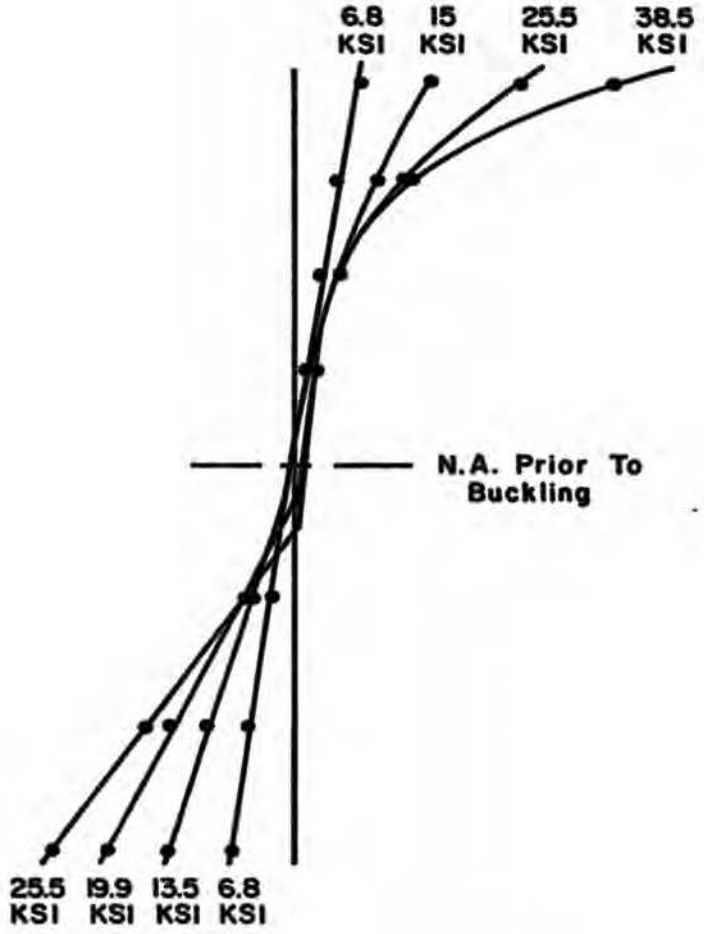

FIG. 5. - Web Stress Distributions at Loads Equal to 26, 51, 77, and 100 % of Ultimate Load for Specimen A3 (h/t = 301)

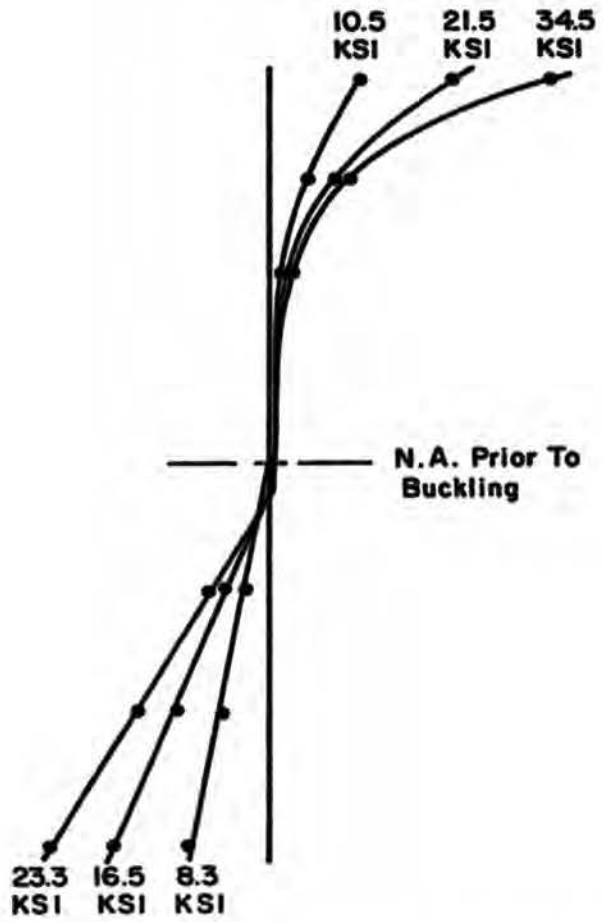

FIG. 6. - Web Stress Distributions at Loads Equal to 34, 67, and 98 % of Ultimate Load for Specimen A4 (h/t = 361)

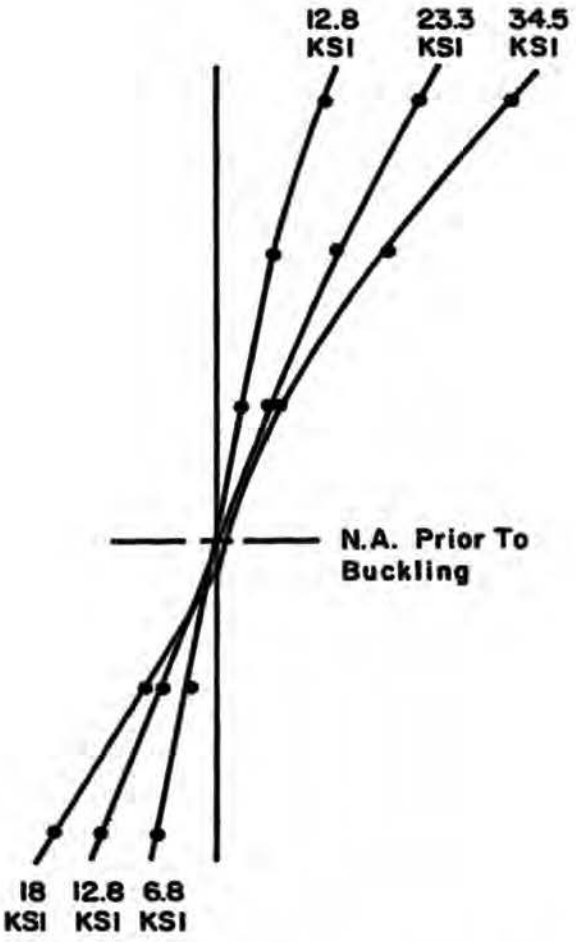

FIG. 7. - Web Stress Distributions at Loads Equal to 32, 64, and 96 % of Ultimate Load for Specimen B1 (h/t = 134)

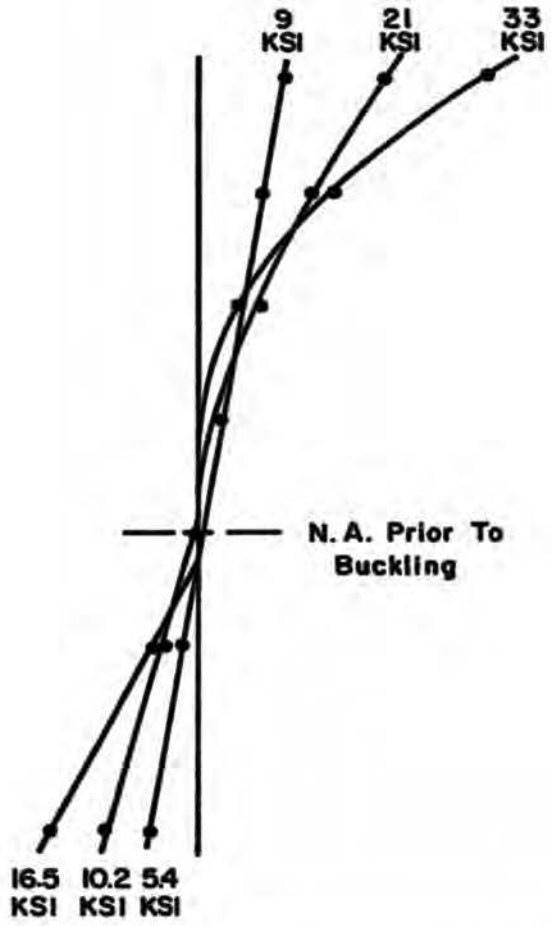

FIG. 8. - Web Stress Distributions at Loads Equal to 33, 67, and 100 % of Ultimate Load for Specimen B2 (h/t = 210)

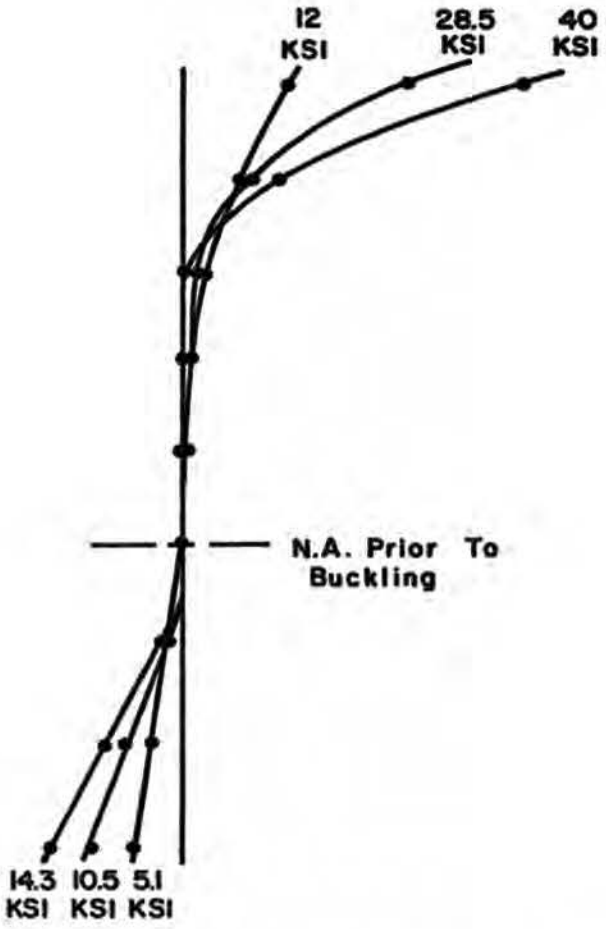

FIG. 9. - Web Stress Distributions at Loads Equal to 33, 67, and 100 % of Ultimate Load for Specimen B3 (h/t = 285)

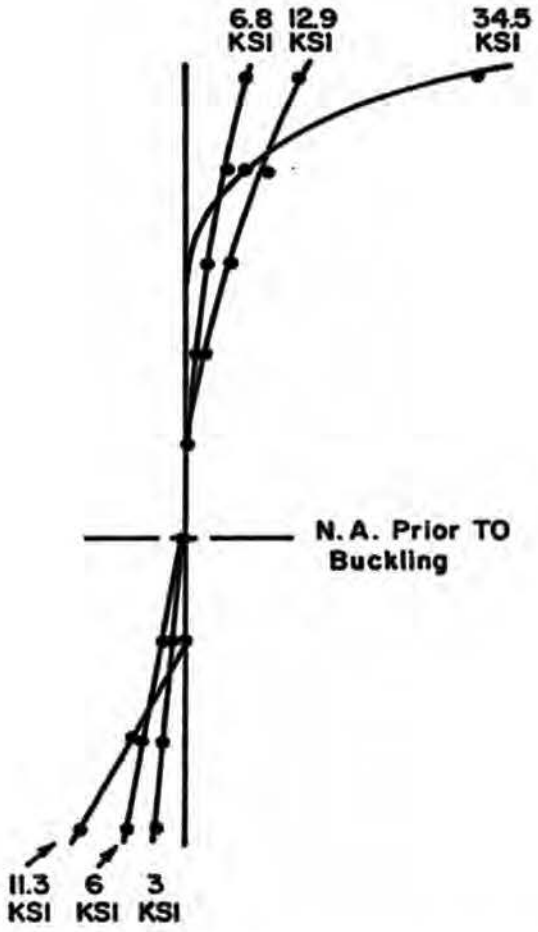

FIG. 10. - Web Stress Distributions at Loads Equal to 32, 64, and 100 % of Ultimate Load for Specimen B4 (h/t = 361)

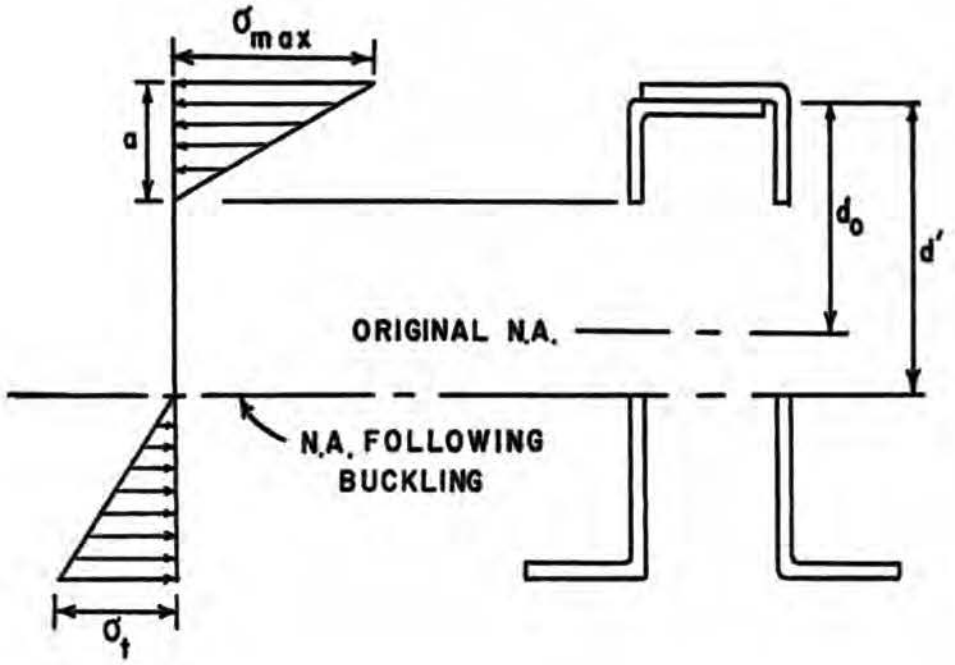

FIG. 11. - Effective Section Used in Proposed Analytical Method

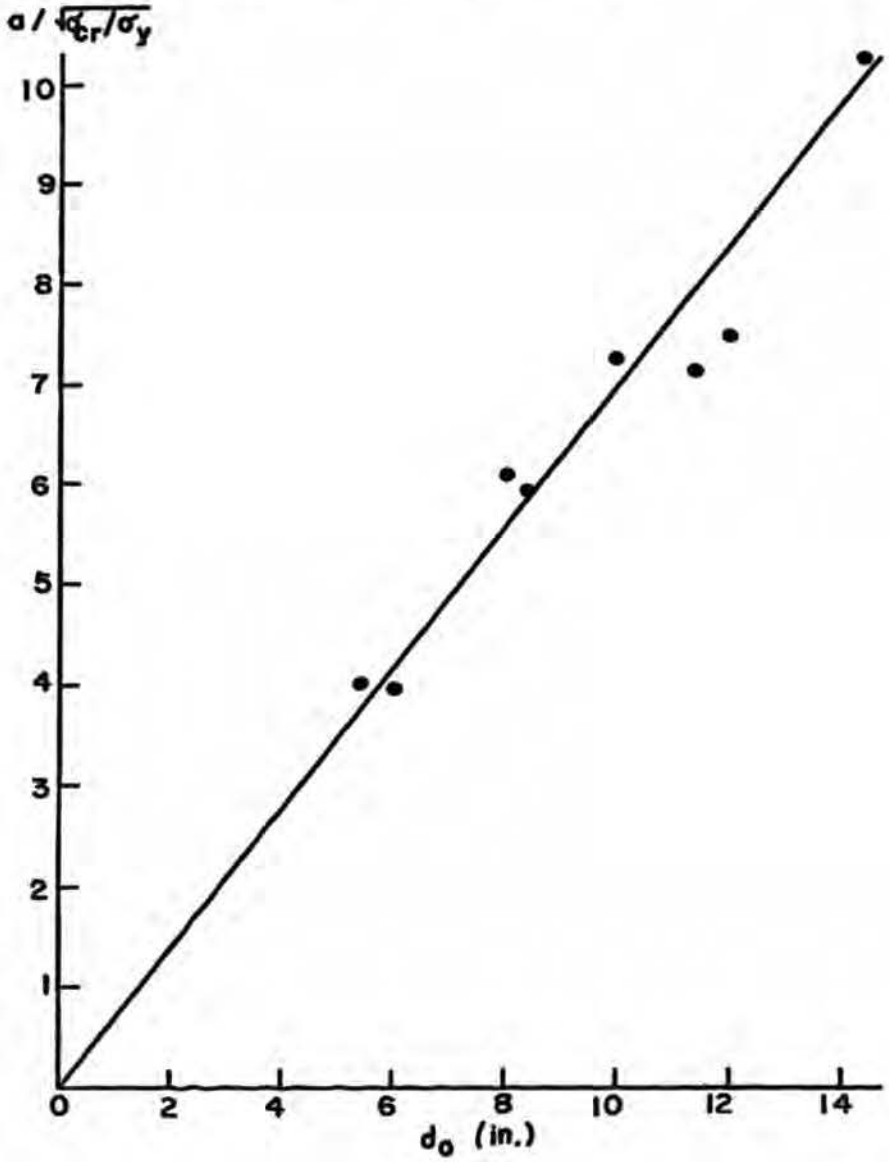

FIG. 12. - Relation Between Effective Width and Depth of Web Compression Zone